Pion spectra for (p,π^-) reactions in the ^{88}Sr region

Shiho Yamamoto and Kenji Kume
Department of Physics, Nara Women's University, Nara 630-8506, Japan
(Received 19 July 1999; published 18 January 2000)

We have calculated the pion spectra of (p,π^-) reactions from near threshold to the Δ region for medium-heavy nuclei with the zero-range plane-wave approximation supplemented with the cutoff of a radial integral simulating the distortion effect. The shell-model wave function with a $1p_{1/2}$-$0g_{9/2}$ configuration is used to calculate the two-particle one-hole spectroscopic amplitudes. The excitation spectra leading to both the positive- and the negative-parity states are calculated for ^{88}Sr, ^{90}Zr, and ^{92}Mo nuclei. The present model calculation predicts pronounced selectivity of the excitation of several high-spin states, especially at higher incident energies.

PACS number(s): 25.40.Qa, 21.60.Cs, 27.50.+e, 27.60.+j

I. INTRODUCTION

In near threshold (p,π^-) reactions, it is well known that the high-spin states are selectively excited due to the large momentum and the angular momentum transfer to the nucleus [1,2]. The high-spin states with dominant two-particle one-hole (2p-1h) stretched configurations with respect to the target nucleus, located at an excitation energy of a few MeV, are strongly populated in the near-threshold (p,π^-) reactions [3,4]. These selective excitations were observed for $f_{7/2}$-shell nuclei [5] and for ^{88}Sr [6]. Brown and co-workers have made zero-range plane-wave calculations with a radial cutoff and have shown that the relative strengths of the pion spectra at a specific angle can be well explained for $f_{7/2}$-shell nuclei [7]. After their work, we have made finite-range distorted-wave calculations with a two-nucleon pion production mechanism, showing that the reaction cross section and the characteristic pattern of the asymmetry for stretched-state transitions are well explained [8–10]. In order to see the details, we have also calculated the separate contribution from the final two-proton state with definite relative angular momentum. We have demonstrated that the (p,π^-) reaction proceeds dominantly through a two-body process $p+n\rightarrow pp(^1S_0)+\pi^-$ with maximal center-of-mass angular momentum for the final two protons which couples to the angular momentum of the neutron hole state, resulting in the 2p-1h stretched configuration [11]. The final two-proton channel $pp(^1S_0)$ is favored due to the high-q nature of this reaction, and this seems to be the reason for the success of the zero-range calculation for the prediction of relative cross sections.

However, the (p,π^-) reaction is not yet thoroughly understood. For ground-state transition for ^{12}C, for example, the Δ peak in the cross section is not clearly observed, which contradicts the theoretical prediction [12,13]. To clarify the mechanism of the (p,π^-) reactions, pertinent experiments are planned at RCNP Osaka at higher energies. Thus, it is both worthwhile and interesting to calculate the (p,π^-) cross sections for the medium-heavy nuclei and predict the pion spectra. In order to predict the energy dependence of the cross sections, it is necessary to carry out the distorted-wave calculations. However, as will be discussed in Sec. III, several hundreds of final states are involved in the present $1p_{1/2}$-$0g_{9/2}$ shell-model calculations. Rather than making tedious distorted-wave calculations for all of these states, it is preferable to make simpler plane-wave calculations first.

Furthermore, it is shown that the zero-range plane-wave approximation with the radial cutoff is successful for explaining the relative cross section for $f_{7/2}$-shell nuclei near threshold [7]. It is not obvious that it works at higher-energy region. To examine the reliability of the plane-wave approximation with radial cutoff, we have made a zero-range plane-wave calculation for $f_{7/2}$-shell nuclei at higher energy regions and compared them with those of finite-range distorted-wave calculations in Ref. [10]. We found that the zero-range calculation gives similar relative strengths with those of the distorted-wave approximation. Since the major purpose of the present work is to predict the overall features of the relative excitation spectra, we adopt the zero-range plane-wave approximation supplemented with a radial cutoff which simulate the distortion effects.

The pion spectra are calculated for the reactions ^{88}Sr$(p,\pi^-)^{89}$Zr, ^{90}Zr$(p,\pi^-)^{91}$Mo, and ^{92}Mo$(p,\pi^-)^{93}$Ru. The inert ^{88}Sr core is assumed, and the 2p-1h specroscopic amplitudes are calculated with the $1p_{1/2}$-$0g_{9/2}$ shell-model wave function due to Serduke *et al.* [14,15].

For the near-threshold ^{88}Sr$(p,\pi^-)^{89}$Zr reaction, the calculation has already been made with the zero-range plane-wave approximation [6], where a single orbit $0g_{9/2}$ shell-model space is used and then the negative-parity states are excluded. In the present work, the $1p_{1/2}$-$0g_{9/2}$ shell-model wave functions are used, and hence both the positive- and negative-parity states are predicted.

For all of the reactions which are of interest here, it is shown that the maximal or nearly maximal high-spin states $\frac{25}{2}^+$ and $\frac{21}{2}^+$ are strongly excited due to better momentum and angular momentum matching. In the $1p_{1/2}$-$0g_{9/2}$ shell-model space, there are a number of high-spin states, but it is interesting that the reaction strengths are strongly concentrated on a single state for each spin: in all of the reactions considered here, the cross sections are considerably large for $(\frac{25}{2}^+)_1$, $(\frac{21}{2}^+)_2$, and $(\frac{17}{2}^+)_3$ states. This concentration of the reaction strengths was also seen for the case of $f_{7/2}$-shell nuclei.

The present paper is organized as follows. In Sec. II, we briefly describe the zero-range plane-wave approximation adopted in the present work. The results are shown and discussed in Sec. III. A summary is given in Sec. IV.

II. REACTION CROSS SECTION

We briefly describe the zero-range plane-wave approximation used to calculate the (p,π^-) reaction cross section. The plane-wave calculation of (p,π^-) reactions, carried out by Brown *et al.* [7], successfully explained the overall features and relative strengths of the reaction spectra for $f_{7/2}$-shell nuclei. In the present work, we assume a similar but slightly different zero-range plane-wave approximation for the calculation of the relative (p,π^-) cross section.

We restrict ourselves to the case of spinless target nuclei. The (p,π^-) reaction amplitude can be written as

$$T(I'I'_z,\mathbf{k}{:}\mathbf{p}\lambda)=\sum \frac{1-(1-\sqrt{2})\delta_{j_bj_c}}{\sqrt{2}}\langle (j_b\otimes j_c)_A^{I_fM_f}|O_\pi|j_a-m_a\mathbf{p}\lambda\rangle(-)^{j_a-m_a}$$
$$\times(j_aI_fm_aM_f|I'I'_z)(-)^{I_f+j_a+I'}\frac{1}{\sqrt{2I'+1}}S_{I'}(I_f{:}j_aj_bj_c), \tag{1}$$

where I' and I'_z are the spin and its z projection of the final nucleus. The momentum and the spin projection of the incident proton are denoted as $\mathbf{p}$ and λ. The symbol (j_am_a) is the quantum number of the neutron-hole state. In the following, symbols such as j_a represent all the quantum numbers $(n_aj_al_a)$ which are necessary to specify the single-particle orbits. (j_bm_b) and (j_cm_c) are the quantum numbers for final two protons. The 2p-1h spectroscopic amplitude $S_{I'}(I_f{:}j_aj_bj_c)$ is defined as

$$S_{I'}(I_f{:}j_aj_bj_c)=\langle I'||\{[a^\dagger_{j_b}\otimes a^\dagger_{j_c}]^{I_f}\otimes b^\dagger_{j_a}\}^{I'}||I=0\rangle, \tag{2}$$

where $a^\dagger_{j_b}$ and $b^\dagger_{j_a}$ are the proton and the neutron-hole creation operators, respectively. For the pion-production operator O_π, we assumed the zero-range interaction of the δ function type. This automatically selects the spin-singlet component for the final two-proton state. In the finite-range distorted-wave calculation, we have shown that the final channel $pp(^1S_0)$ dominates the reaction cross section. Though the spin-triplet $pp(^3P)$ component gives a non-negligible contribution for the asymmetry distribution, our major concern here is to predict the overall feature of the reaction spectrum, and we think that the zero-range approximation is enough for this purpose. We assumed the operator to have the following form:

$$O_\pi=\sum_{i>j}\delta(\mathbf{r}_i-\mathbf{r}_j)e^{-i\mathbf{k}\cdot\mathbf{r}_i}\mathbf{\Sigma}^{(S)}\cdot\mathbf{A}^{(S)}, \tag{3}$$

where $\mathbf{\Sigma}^{(S)}$ is the operator of rank S acting on the two-nulceon spin coordinates and $A^{(S)}$ is the c-number quantity. The reaction amplitude can be written as

$$T(I'I'_z,\mathbf{k}{:}\mathbf{p}\lambda)=\sum_{lNN_zS}(-1)^{I'+S+\lambda}W\left(\frac{1}{2}\frac{1}{2}Nl{:}SI'\right)(-)^{N_z}[Y_l(\mathbf{q})\otimes A^{(S)}]^{N-N_z}$$
$$\times\left(\frac{1}{2}I'-\lambda I'_z\middle|NN_z\right)\langle 0||\Sigma^{(S)}||S\rangle F(l{:}q), \tag{4}$$

where $\langle 0||\Sigma^{(S)}||S\rangle$ is the reduced matrix element of the two nucleon spins. We define the amplitude $F(l{:}q)$ as

$$F(l{:}q)=\sum_{I_f}\sum_{j_aj_bj_c}(-)^{j_a+j_b+l_c+1}\sqrt{\frac{(2j_a+1)(2j_b+1)(2j_c+1)}{2(2I_f+1)}}$$
$$\times\left(j_bj_c\frac{1}{2}-\frac{1}{2}\middle|I_f0\right)\left(I'j_a\frac{1}{2}-\frac{1}{2}\middle|I_f0\right)\Delta(l_bl_cI_f)\Delta(ll_aI_f)$$
$$\times S_{I'}(I_f{:}j_aj_bj_c)i^l\int_0^\infty j_l(qr)R_{j_a}(r)R_{j_b}(r)R_{j_c}(r)r^2dr, \tag{5}$$

with

$$\Delta(l_b l_c I_f)=\begin{cases}1 & \text{for } |l_b-l_c|\leqslant I_f\leqslant l_b+l_c \quad \text{and} \quad l_b+l_c+I_f=\text{even}\\ 0, & \text{otherwise.}\end{cases} \tag{6}$$

$R_{j_a}(r)$'s are the radial parts of the single-particle wave functions. Because of the parity conservation, the terms with $S=0$ and $S=1$ do not interfere. Then, there appear the terms proportional to $[Y_L(\hat{\mathbf{q}})\otimes(A^{(S)}\otimes A^{(S)})^L]^0$. The angular momentum conservation coming from the Racah coefficient restricts L to be 0 and 1, only $L=0$ term giving a non-negligible contribution. Neglecting the angular dependence of the quantity $A^{(S)}$, the relative reaction cross section can be written as

$$\frac{d\sigma}{d\Omega}=\text{const}\sum_l |F(l{:}q)|^2, \tag{7}$$

where l is the orbital angular-momentum transfer to the nucleus which takes the values $l=I'\pm\frac{1}{2}$. Because of the parity conservation, a single l value is relevant in each transition. In order to simulate the distortion effects, we discarded the radial integral in Eq. (5) up to cutoff radius R_c, which is determined to reproduce the angular distribution of the cross sections leading to high-spin states.

III. RESULTS AND DISCUSSIONS

According to the formulas described in Sec. II, we have calculated the (p,π^-) reaction cross section for the nuclei in the ^{88}Sr region. Previously, the reaction spectra near threshold were calculated for ^{88}Sr [6], but these calculations assumed the single $0g_{9/2}$ shell-model wave function, thus the negative-parity states are excluded. In the present work, we employed a $1p_{1/2}$-$0g_{9/2}$ shell-model wave function with an inert ^{88}Sr core and then predicted the excitation of the final states with both positive- and negative-parity states. We have considered the $N=50$ isotones ^{88}Sr, ^{90}Zr, and ^{92}Mo for the target nuclei. The final states are isotones with a single neutron hole $N=49$. The shell-model wave functions for these nuclei are calculated with the effective interaction by Serduke and co-workers [14,15] and are used to calculate the 2p-1h spectroscopic amplitudes in Eq. (2). For the reactions ^{88}Sr$(p,\pi^-)^{89}$Zr, ^{90}Zr$(p,\pi^-)^{91}$Mo, and ^{92}Mo$(p,\pi^-)^{93}$Ru, the $1p_{1/2}$-$0g_{9/2}$ shell model gives 69, 401, and 696 final states, respectively. For the residual nuclei, the maximal spins are $\frac{25}{2}^+$ and $\frac{19}{2}^-$ for the positive- and the negative-parity states. We used the harmonic-oscillator radial wave function with oscillator parameter 2.12 fm. To simulate the strong pion absorption, we discarded the radial overlap integral up to $R_c=3.3$ fm, which reproduces well the experimental angular distributions of the cross sections for $(\frac{25}{2}^+)_1$ and $(\frac{21}{2}^+)_2$ states for the reaction ^{88}Sr$(p,\pi^-)^{89}$Zr [4]. This value is slightly smaller than that used by Brown *et al.* [7]. We used this cutoff radius throughout irrespective of the incident proton energies. The angular distributions of the cross sections are shown in Fig. 1 for the case of ^{90}Zr for incident proton energy $T_p=200$ MeV. At higher energies, the cross section can be obtained by scaling with respect to the momentum transfer q. The results of the pion spectra at 30° are shown in Figs. 2–4 for various incident energies. Since the absolute values of the cross section cannot be predicted in the present plane-wave calculations, the reaction spectra are shown such that the dominant peak for the transition ^{88}Sr$(p,\pi^-)^{89}$Zr$[(\frac{21}{2}^+)_2{:}3.67\ \text{MeV}]$ is 1 for all the incident energies. We can compare the relative reaction strengths for ^{88}Sr, ^{90}Zr, and ^{92}Mo nuclei. However, the relative reaction strengths for different energies in Figs. 2–4 cannot be compared. In order to predict the absolute value of the cross sections, the polarization observables, and their energy dependences, it is necessary to carry out the finite-range distorted-wave calculations assuming a specific reaction mechanism. In these figures, the vertical solid lines correspond to the excitation of positive-parity states, while the dashed ones are for the negative-parity states. The high-spin states $\frac{25}{2}^+$ and $\frac{21}{2}^+$ are predominantly excited for all of these nuclei. The angular momentum conservation requires $I'=l\pm\frac{1}{2}$ for a spinless target. Then a single l value is relevant for each transition due to parity conservation. As was pointed out by Brown *et al.* [7], the states with $I'=l+\frac{1}{2}$ are more strongly populated than those with $I'=l-\frac{1}{2}$ because of the transformation from LS to jj scheme. The $\frac{25}{2}^+$ and $\frac{21}{2}^+$ states correspond to $l=12$ and $l=10$ with $I'=l+\frac{1}{2}$. The $\frac{23}{2}^+$ states correspond to $l=12$ with $I'=l-\frac{1}{2}$ and are weakly populated. For negative-parity single-hole states in a $1p_{1/2}$-$0g_{1/9}$ model space, the $1p_{1/2}$ orbit is necessarily involved and the maximal spin is $\frac{19}{2}^-$. In this case, $\frac{19}{2}^-$ states

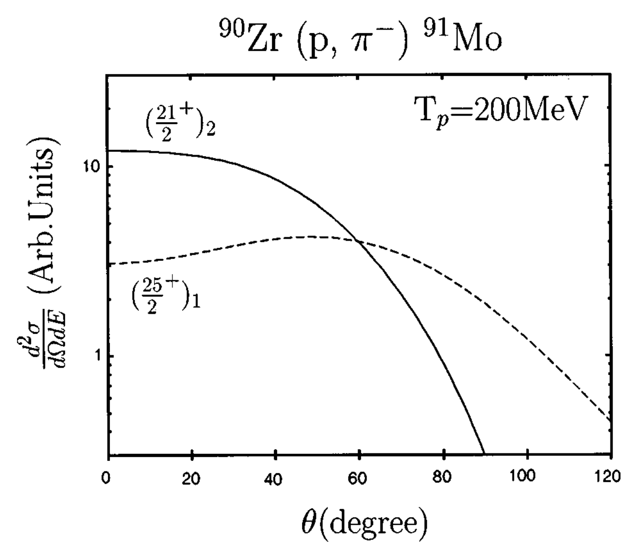

FIG. 1. The angular distributions of the cross sections for ^{90}Zr$(p,\pi^-)^{91}$Mo, leading to $(\frac{25}{2}^+)_1$ and $(\frac{21}{2}^+)_2$ states. The cutoff radius $R_c=3.3$ fm is used to evaluate the radial overlap integral.

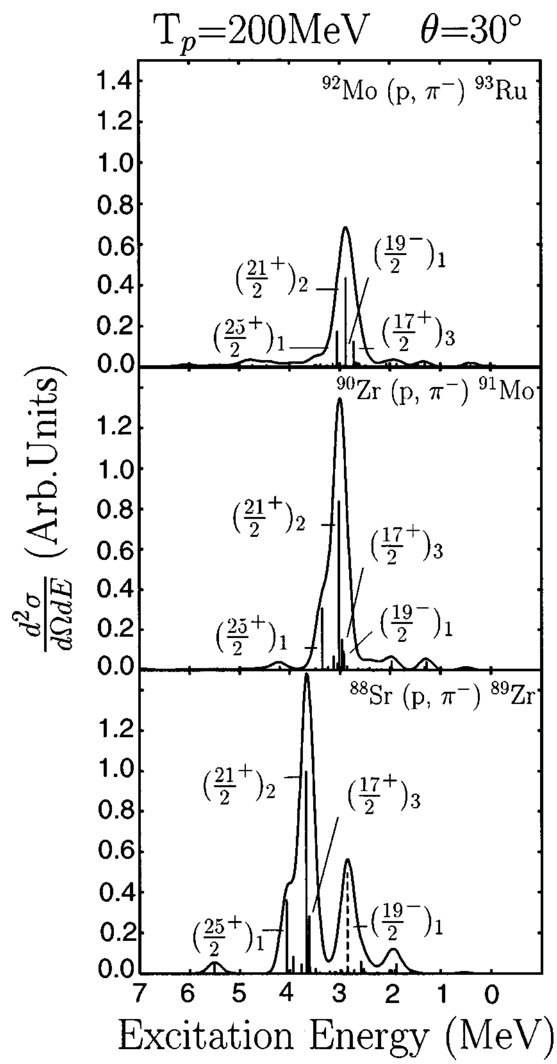

FIG. 2. The pion spectra for (p,π^-) reactions on ^{88}Sr, ^{90}Zr, and ^{92}Mo at incident energy $T_p = 200$ MeV. The vertical lines represent the final state with positive parity, while the dashed ones are those with negative parity. The solid curves are Gaussian average with $\Gamma_{\rm FWHM} = 0.3$ MeV.

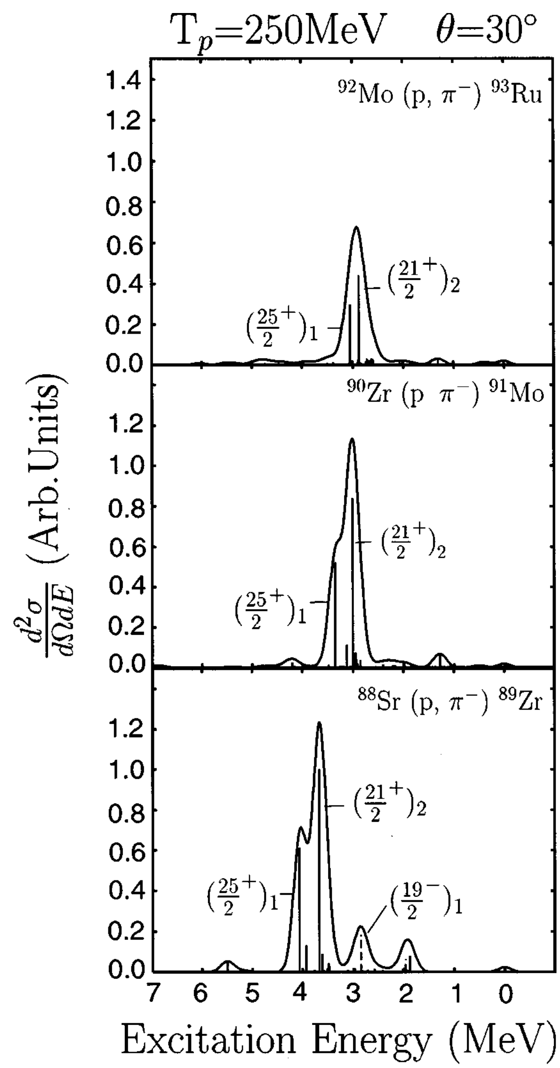

FIG. 3. The pion spectra for (p,π^-) reactions on ^{88}Sr, ^{90}Zr, and ^{92}Mo. The curves are the same as in Fig. 1 but at the incident proton energy $T_p = 250$ MeV.

correspond to $l=9$ with $I' = l + \frac{1}{2}$. The negative-parity states are rather weakly populated, and only a prominent peak is $(\frac{19}{2}^-)_1$ state at low incident energy. It is interesting to note that, for specific spin states, the reaction strengths are concentrated on a single state for each spin. In all of the reactions considered here, the final states $(\frac{25}{2}^+)_1$, $(\frac{21}{2}^+)_2$, $(\frac{17}{2}^+)_3$, and $(\frac{19}{2}^-)_1$ are strongly excited.

For a detailed description, we have listed the 2p-1h spectroscopic amplitudes for the ^{90}Zr$(p,\pi^-)^{91}$Mo reaction in Table I. As can be seen for the transitions leading to $\frac{25}{2}^+$ states, the spectroscopic amplitude is large for the first $(\frac{25}{2})_1^+$ state. The ground-state wave function of the ^{90}Zr nucleus is

$$0.815|(p_{1/2}^2)^0\rangle - 0.580|(g_{9/2}^2)^0\rangle, \tag{8}$$

and the final $\frac{25}{2}^+$ state of ^{91}Mo has shell-model configurations $|(g_{9/2}^4)g_{9/2}^{-1}\rangle$ or $|(p_{1/2}^2)(g_{9/2}^2)g_{9/2}^{-1}\rangle$. The first and third $\frac{25}{2}^+$ states have large components $|[(g_{9/2}^4)^8 g_{9/2}^{-1}]^{25/2}\rangle$ or $|[(p_{1/2}^2)^0(g_{9/2}^2)^8 g_{9/2}^{-1}]^{25/2}\rangle$ and this leads to the transitions

$$|(p_{1/2}^2)^0\rangle \rightarrow |[(p_{1/2}^2)^0(g_{9/2}^2)^8 g_{9/2}^{-1}]^{25/2}\rangle,$$

$$|(g_{9/2}^2)^0\rangle \rightarrow |[(g_{9/2}^4)^8 g_{9/2}^{-1}]^{25/2}\rangle, \tag{9}$$

these contributions interfering constructively for the $(\frac{25}{2}^+)_1$ state and destructively for the $(\frac{25}{2}^+)_2$ state, resulting in the large 2p-1h spectroscopic amplitudes for the $(\frac{25}{2}^+)_1$ state shown in Table I.

The similar interference takes place for the transitions to $\frac{21}{2}^+$ states. In this case, there are 13 final $\frac{21}{2}^+$ states with configurations of the following types: $|(p_{1/2})(g_{9/2}^3)p_{1/2}^{-1}\rangle$, $|(g_{9/2}^4)g_{9/2}^{-1}\rangle$ and $|(p_{1/2}^2)(g_{9/2}^2)g_{9/2}^{-1}\rangle$. The low-lying $\frac{21}{2}^+$ states have large components: $|(p_{1/2}^2)^0(g_{9/2}^2)^6 g_{9/2}^{-1}\rangle$, $|(p_{1/2}^2)^0(g_{9/2}^2)^8 g_{9/2}^{-1}\rangle$, $|(g_{9/2}^4)^6 g_{9/2}^{-1}\rangle$, and $|(g_{9/2}^4)^8 g_{9/2}^{-1}\rangle$. Then, various transition amplitudes interfere,

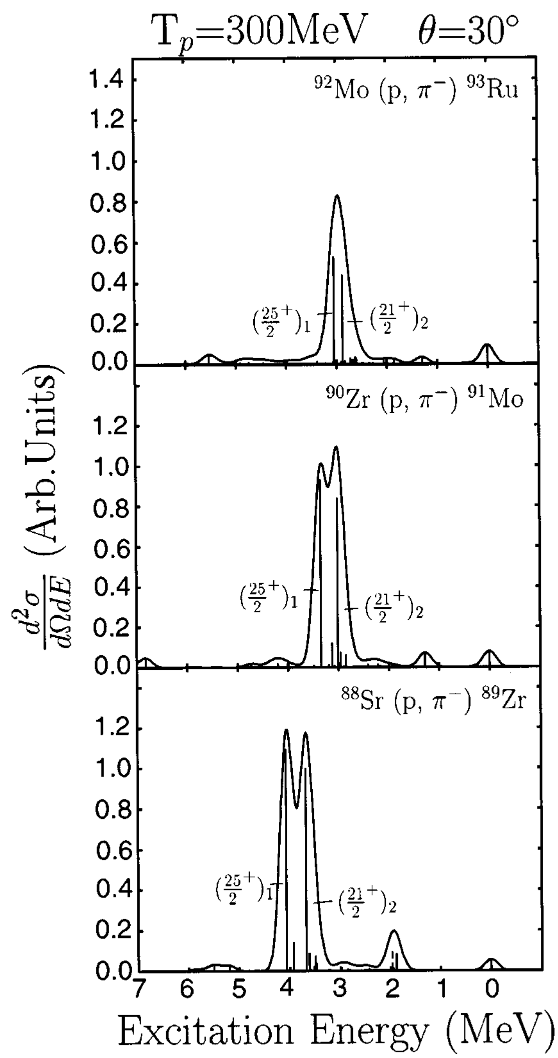

FIG. 4. The pion spectra for (p,π^-) reactions on ^{88}Sr, ^{90}Zr, and ^{92}Mo. The curves are the same as in Fig. 1 but at the incident proton energy $T_p=300$ MeV.

giving large 2p-1h amplitudes for $(\frac{21}{2}^+)_1$ and $(\frac{21}{2}^+)_2$ states, as seen in Table I. Furthermore, the two transition amplitudes corresponding to the spectroscopic amplitudes $S_{I'}(I_f=6)$ and $S_{I'}(I_f=8)$ interfere with each other, and the cross sections are quite large for the $(\frac{21}{2}^+)_2$ state, as seen in Figs. 2–4. A similar situation occurs in almost all of the transitions leading to high-spin states. For each spin state, the reaction strengths are concentrated on a single state: $(\frac{25}{2}^+)_1$ (about 98%), $(\frac{21}{2}^+)_2$ (about 96%) for ^{90}Zr. Thus, among hundreds of final states, only a limited number of high-spin states are selectively excited.

For the isotones considered here, the proton occupancy in the $1p_{1/2}$-$0g_{9/2}$ shell increases with the increase of mass number, and the pion spectra are less pronounced for heavier targets. At higher energies, the selective excitation of the high-spin states is more pronounced due to large momentum and angular momentum mismatch.

TABLE I. The 2p-1h spectroscopic amplitudes $S_{I'}(I_f:j_a=j_b=j_c=\frac{9}{2})$ for the reaction ^{90}Zr$(p,\pi^-)^{91}$Mo.

$\frac{25}{2}^+$	Excitation energy	$S_{I'}(I_f=8)$
	3.347 33	−5.3773
	4.387 24	−0.2575
	4.728 43	−0.6210
	5.254 19	−0.0634
	5.844 84	−0.1539
	6.324 72	−0.1772

$\frac{21}{2}^+$	Excitation energy	$S_{I'}(I_f=8)$	$S_{I'}(I_f=6)$
	2.166 52	2.6553	−4.3480
	3.011 37	−3.8197	−3.1034
	3.483 21	−0.6079	−0.0414
	4.237 30	0.2426	0.1115
	4.438 40	−0.2908	−0.1202
	4.633 69	−0.0120	−0.0993
	4.897 24	−0.1635	0.1920
	5.344 37	−0.0396	−0.2632
	5.545 64	−0.3011	0.1544
	5.803 76	−0.0351	−0.3473
	6.047 70	−0.2268	0.1613
	7.043 77	0.2545	−0.2626
	10.37 84	0.3349	−0.7114

IV. SUMMARY

We have calculated the pion spectra for (p,π^-) reactions on medium-heavy nuclei ^{88}Sr, ^{90}Zr, and ^{92}Mo with zero-range plane-wave approximation. The pion absorption effects are approximately taken into account by cutting off the inner part of the radial overlap integral. The shell-model wave functions with $1p_{1/2}$-$0g_{9/2}$ model space are used to calculate the 2p-1h spectroscopic amplitudes. We could predict the reaction cross sections leading to low-lying positive- and negative-parity states. For these nuclei, the $(\frac{21}{2}^+)_2$ and $(\frac{25}{2}^+)_1$ states are strongly excited. The 2p-1h spectroscopic amplitudes are fairly large for a single or several states. Moreover, due to the interference between these amplitudes, the resulting reaction strengths are strongly concentrated on a single state for each spin. For the case of ^{88}Sr, the negative-parity state $\frac{19}{2}^-$ is expected to be appreciably excited as well. The selectivity of the excitation of high-spin states is pronounced at higher energy region due to the large momentum and angular momentum mismatch. It is our hope that the completion of the (p,π^-) experiment around these nuclei sheds light on the reaction mechanism.

ACKNOWLEDGMENTS

We would like to thank Professor K. Hatanaka and Dr. N. Nose-Togawa for stimulating discussions. This work was supported by a Grant-in-Aid for Scientific Research (No. 08640376) from the Japan Ministry of Education, Science, and Culture.

[1] D.F. Measday and G.A. Miller, Annu. Rev. Nucl. Part. Sci. **29**, 121 (1979).
[2] H.W. Fearing, *Progress in Particle and Nuclear Physics*, edited by D. Wilkinson (Pergamon, Oxford, 1981), Vol. 7, p. 113.
[3] S.E. Vigdor *et al.*, Phys. Rev. Lett. **49**, 1314 (1982).
[4] Z.-J. Cao, R.-D. Bent, H. Nann, and T.E. Ward, Phys. Rev. C **35**, 625 (1987).
[5] T.G. Throwe, S.E. Vogdor, W.W. Jacobs, M.C. Green, C.W. Glover, T.E. Ward, and B.P. Hichwa, Phys. Rev. C **35**, 1083 (1987).
[6] M.C. Green, P.L. Jolivette, and B.A. Brown, Phys. Rev. Lett. **53**, 1893 (1984).
[7] B.A. Brown, O. Scholten, and H. Toki, Phys. Rev. Lett. **51**, 1952 (1983).
[8] K. Kume, Nucl. Phys. **A504**, 712 (1989).
[9] K. Kume, Nucl. Phys. **A511**, 701 (1990).
[10] N. Nose, K. Kume, and H. Toki, Phys. Rev. C **53**, 2324 (1996).
[11] K. Kume, Phys. Lett. B **271**, 17 (1991).
[12] G.M. Huber, G.J. Lolos, R.D. Bent, K.H. Hicks, P.L. Walden, S. Yen, X. Aslanoglou, E.G. Auld, and W.R. Falk, Phys. Rev. C **37**, 1161 (1988).
[13] N. Nose, K. Kume, and H. Toki, Phys. Rev. C **57**, 2502 (1998).
[14] F.J.D. Serduke, D.H. Lawson, and D.H. Gloeckner, Nucl. Phys. **A256**, 45 (1976).
[15] D.H. Gloeckner and F.J.D. Serduke, Nucl. Phys. **A220**, 477 (1974).